

Combined $t\bar{t}$ Production Cross Section at $\sqrt{s} = 1.96$ TeV in the Lepton+Jets and Dilepton Final States using Event Topology

DØ collaboration
(Dated: August 24, 2005)

Measurements of the $t\bar{t}$ production cross-section at $\sqrt{s} = 1.96$ TeV, based on the application of a topological method to data preselected in the e +jets (226.3 pb^{-1}), μ +jets (229.1 pb^{-1}), ee (243.0 pb^{-1}), $e\mu$ (228.3 pb^{-1}) and $\mu\mu$ (224.3 pb^{-1}) channels have recently become available. In this note we present a combination of these measurements. The combined cross section in lepton+jet channel is found to be:

$$\ell + \text{jets} : \quad \sigma_{t\bar{t}} = 6.7^{+1.4}_{-1.3} \text{ (stat)} \quad {}^{+1.6}_{-1.1} \text{ (syst)} \quad \pm 0.4 \text{ (lumi)} \text{ pb}$$

while the combined cross section in dilepton channel yields

$$\text{dilepton} : \quad \sigma_{t\bar{t}} = 8.6^{+3.2}_{-2.7} \text{ (stat)} \quad {}^{+1.1}_{-1.1} \text{ (syst)} \quad \pm 0.6 \text{ (lumi)} \text{ pb.}$$

The combined cross section in dilepton and lepton+jet channels is estimated to be:

$$\sigma_{t\bar{t}} = 7.1^{+1.2}_{-1.2} \text{ (stat)} \quad {}^{+1.4}_{-1.1} \text{ (syst)} \quad \pm 0.5 \text{ (lumi)} \text{ pb.}$$

I. INTRODUCTION

The measurements of the $t\bar{t}$ production cross section at $\sqrt{s} = 1.96$ TeV, based on the application of a topological method to data selected in the e +jets (226.3 pb^{-1}) and μ +jets (229.1 pb^{-1}) channels are summarized in Refs [1] and [2], respectively. The measurements of the $t\bar{t}$ production cross section at $\sqrt{s} = 1.96$ TeV utilizing approximately 230 pb^{-1} of data selected in ee , $e\mu$ and $\mu\mu$ channels are described in Refs [3]. In this note we present combinations of the cross sections measured in individual channels.

II. METHOD

A. Dilepton channels

To estimate cross section σ_j in a dilepton channel j the following likelihood function is defined:

$$L(\sigma_j, \{N_j^{obs}, N_j^{bkg}, BR_j, \mathcal{L}_j, \epsilon_j\}) = \mathcal{P}(N_j^{obs}, \mu_j) = \frac{\mu_j^{N_j^{obs}}}{N_j^{obs}!} e^{-\mu_j}, \quad (1)$$

where $\mathcal{P}(N_j^{obs}, \mu_j)$ is the Poisson probability of expected μ_j signal-plus-background events:

$$\mu_j = \sigma_j BR_j \mathcal{L}_j \epsilon_j + N_j^{bkg} \quad (2)$$

to be compatible with the number of observed events N_j^{obs} given the luminosity \mathcal{L}_j , branching fraction BR_j , efficiency ϵ_j and expected number of background events N_j^{bkg} . The cross section in individual channel is extracted by minimizing the negative log-likelihood function, $-\log L(\sigma_j, \{N_j^{obs}, N_j^{bkg}, BR_j, \mathcal{L}_j, \epsilon_j\})$, while the combined cross section from n channels is estimated by minimizing the sum of the negative log-likelihood functions for each individual channel:

$$-\log L(\sigma, \{N_j^{obs}, N_j^{bkg}, BR_j, \mathcal{L}_j, \epsilon_j\}_{j=1\dots n}) \approx \sum_{j=1}^n (-N_j^{obs} \log \mu_j + \mu_j) \quad (3)$$

where on the right hand side any terms independent of σ have been dropped. The number of observed events, the estimated background, the $t\bar{t}$ selection efficiency, the decay branching fraction for the $t\bar{t}$ final state where leptons are allowed to originate either directly from a W or from $W \rightarrow \tau\nu$ decay, as derived from [4], and the integrated luminosity for each channel are summarized in Table 1.

channel	Observed	N^{bkg}	BR	\mathcal{L} (pb^{-1})	ϵ
ee	5	0.93	0.01584	243.00	0.071
$e\mu$	8	0.91	0.03155	228.29	0.102
$\mu\mu$	0	1.37	0.01571	224.33	0.063

TABLE 1: Number of observed events, estimated background, $t\bar{t}$ selection efficiency, decay branching ratio for $t\bar{t} \rightarrow l\bar{l}' + X$, and integrated luminosity for each channel.

B. Lepton+jets channels

The method used to calculate the cross sections in the individual channels is described in Section VII of Refs. [1] and [2]. Here we give again an overview.

In a particular lepton+jets channel, the composition of the preselected data sample is dominated by three sources: W +jets and multijets (in the following denoted as QCD) backgrounds, and the $t\bar{t}$ signal. In order to extract the $t\bar{t}$ contribution, a discriminant variable is built taking advantage of the differences in event topology between signal and background. We perform a likelihood fit to this discriminant and simultaneously extract the number of $t\bar{t}$ ($N_t^{t\bar{t}}$), W +jets (N_t^W) and QCD (N_t^{QCD}) in the preselected (a.k.a. tight (t)) sample, while constraining N_t^{QCD} to the prediction given by the Matrix Method. The Matrix Method is based on the definition of a sample with less stringent

requirements on the lepton identification criteria (a.k.a. loose (ℓ) sample) than the preselected sample, and makes use of pre-determined efficiencies, ε_{sig} and ε_{QCD} , for a real and fake lepton, respectively, to pass from the loose to the tight sample. For the detailed definition of tight and loose samples and description of the Matrix Method see Sect.V.A of Ref. [1] and Sect.V.B of Ref. [2].

In order to estimate $N_t^{t\bar{t}}$, N_t^W and N_t^{QCD} , the following likelihood function is defined:

$$L(N_t^{t\bar{t}}, N_t^W, N_t^{QCD}) = \left[\prod_i \mathcal{P}(n_i^{obs}, \mu_i) \right] \mathcal{P}(N_{\ell-t}^{obs}, N_{\ell-t}) \quad (4)$$

where $\mathcal{P}(n, \mu)$ denotes the Poisson probability density function for n observed events given an expectation value of μ (Eq. 1). In the first term of Eq. 4, i runs over all bins of the likelihood discriminant histogram, n_i^{obs} is the content of bin i as obtained in the preselected sample, and μ_i is the expectation for bin i , which is a function of $N_t^{t\bar{t}}$, N_t^W and N_t^{QCD} as given by:

$$\mu_i(N_t^{t\bar{t}}, N_t^W, N_t^{QCD}) = f_i^{t\bar{t}} N_t^{t\bar{t}} + f_i^W N_t^W + f_i^{QCD} N_t^{QCD} \quad (5)$$

where $f_i^{t\bar{t}}$, f_i^W , f_i^{QCD} represent the fractions in bin i of the $t\bar{t}$, W and QCD likelihood discriminant templates, respectively. The second term of Eq. 4 effectively implements the Matrix Method constraint on N_t^{QCD} via the Poisson probability of the observed number of events in the loose but not tight ($N_{\ell-t}^{obs}$) sample, given the expectation ($N_{\ell-t}$). The latter can be expressed as:

$$N_{\ell-t} = \frac{1 - \varepsilon_{sig}}{\varepsilon_{sig}} N_t^{t\bar{t}} + \frac{1 - \varepsilon_{sig}}{\varepsilon_{sig}} N_t^W + \frac{1 - \varepsilon_{QCD}}{\varepsilon_{QCD}} N_t^{QCD}. \quad (6)$$

Thus, the task is to minimize the negative log-likelihood function:

$$-\log L(N_t^{t\bar{t}}, N_t^W, N_t^{QCD}) \simeq \sum_i -n_i^{obs} \log \mu_i + \mu_i - N_{\ell-t}^{obs} \log N_{\ell-t} + N_{\ell-t} \quad (7)$$

where any terms independent of the minimization parameters have been dropped. The estimated parameters are given by their value at the minimum and their covariance matrix is obtained by the usual procedure of varying the negative log-likelihood by half unit above the minimum.

The $t\bar{t}$ production cross section for a particular lepton channel j is then computed as:

$$\sigma_j = \frac{N_t^{t\bar{t}}(j)}{\varepsilon_j BR_j \mathcal{L}_j}, \quad (8)$$

where $N_t^{t\bar{t}}(j)$ is the number of fitted $t\bar{t}$ events in channel j , BR_j is the branching fraction [4] for the $t\bar{t}$ final state where the lepton is allowed to originate either directly from a W or from $W \rightarrow \tau\nu$ decay, \mathcal{L}_j is the integrated luminosity and ε_j is the $t\bar{t}$ selection efficiency. The input values for the likelihood fit are summarized in Table 2.

channel	N_t	N_ℓ	BR	\mathcal{L} (pb $^{-1}$)	ε	ε_{sig}	ε_{QCD}
$e + \text{jets}$	230	87	0.17106	226.3	0.1162	0.817	0.16
$\mu + \text{jets}$	148	80	0.17036	229.1	0.1168	0.806	0.085

TABLE 2: Number of selected events in the loose (N_ℓ) and tight (N_t) sample, branching fraction (BR), integrated luminosity (\mathcal{L}), preselection efficiency (ε) and loose-to-tight efficiencies for real (ε_{sig}) and fake (ε_{QCD}) leptons.

The combined cross section in lepton+jets channel [6] is estimated by minimizing the sum of the negative log-likelihood functions for each individual channel. A total of five parameters are simultaneously fitted: $\sigma_{t\bar{t}}$ (common to both lepton channels) and $N_t^W(j)$ and $N_t^{QCD}(j)$ separately for each channel. This requires $N_t^{t\bar{t}}(j)$ in the likelihood expression for each channel to be replaced by $\varepsilon_j BR_j \sigma_j \mathcal{L}_j$.

C. Dilepton and lepton+jets channel combination

In the topological method dilepton data sample is selected to be orthogonal to the lepton+jets sample. Since the samples are statistically independent the combined cross section is obtained by minimizing the sum of the negative

log-likelihood functions of five individual channels: ee , $e\mu$, $\mu\mu$, e +jets and μ +jets. The statistical uncertainty on the combined cross section is obtained by the usual procedure of varying the negative log-likelihood by half unit above the minimum.

The systematic uncertainty on the cross section is obtained for each independent source of systematic, by varying the source by one standard deviation up and down and propagating the variation into both background estimates (in dilepton channels) or fitted number of $t\bar{t}$ events (in lepton+jets channels) and signal efficiencies. A new likelihood function is derived for each such variation to give a new optimal cross section. These variations in the central value of the cross section are then summed quadratically to obtain the total systematic uncertainty. By construction, this method of the cross section computation does not allow the systematic errors to influence the result of the fit.

III. SYSTEMATIC UNCERTAINTIES

The complete list of systematic uncertainties is given in Table 3, where a cross indicates which channels are affected. The systematic uncertainties have been classified as uncorrelated (usually of statistical origin in either Monte Carlo or data) and correlated. This information is used for the combined cross section calculation.

A. Dilepton channel

The systematic uncertainties in the dilepton channels can be subdivided into uncertainties on the signal efficiencies and on the background. The sources of systematic uncertainties affecting the tt selection efficiency (ε) and various backgrounds (relevant in case of the cross section estimation for each individual dilepton channel), are summarized in Tables 4 and 5 for ee , $e\mu$ and $\mu\mu$ channels. Variations due to error sources which contribute to the error on the selection efficiency and on the background, are treated as fully correlated.

B. Lepton+jets channel

The systematic uncertainties on the $t\bar{t}$ production cross section for an individual channel is determined by varying in Eq. 8 the signal efficiencies and the fitted number of $t\bar{t}$ events within their errors. In particular, variations due to error sources which contribute to the error on the preselection efficiency and to the likelihood fit, are treated as fully correlated.

The sources of systematic uncertainties affecting the $t\bar{t}$ selection efficiency (ε) and fitted number of $t\bar{t}$ events ($N_t^{t\bar{t}}$) (relevant in case of the cross section estimation for each individual lepton channel), are summarized in Table 6 for both lepton+jets channels. The systematic uncertainties on $N_t^{t\bar{t}}$ originate from distortions on one or more of the templates used to fit the likelihood discriminant distribution in the data. A detailed discussion can be found in Refs [1] and [2].

IV. RESULTS

A. Dilepton channel

The $t\bar{t}$ production cross sections at $\sqrt{s} = 1.96$ TeV for a top mass of 175 GeV, in dilepton channels are measured to be:

$$\begin{aligned}
 ee & : \quad \sigma_{t\bar{t}} = 14.9_{-7.0}^{+9.4} \text{ (stat)} \quad {}_{-1.8}^{+2.5} \text{ (syst)} \quad \pm 1.0 \text{ (lumi) pb;} \\
 e\mu & : \quad \sigma_{t\bar{t}} = 9.7_{-3.4}^{+4.3} \text{ (stat)} \quad {}_{-1.3}^{+1.2} \text{ (syst)} \quad \pm 0.6 \text{ (lumi) pb;} \\
 ee + e\mu + \mu\mu \text{ combined} & : \quad \sigma_{t\bar{t}} = 8.6 \quad {}_{-2.7}^{+3.2} \text{ (stat)} \quad {}_{-1.1}^{+1.1} \text{ (syst)} \quad \pm 0.6 \text{ (lumi)pb;}
 \end{aligned}
 \tag{9}$$

Table 7 summarizes the contributions from the different sources of systematic uncertainties to the total systematic uncertainty on the cross section in the ee , $e\mu$ and combined dilepton (ee , $e\mu$, $\mu\mu$) channel. Figure 1 shows the dependence of the combined cross section in dilepton channels on top quark mass. In the region 170 GeV to 180 GeV

Channel	ee	$e\mu$	$\mu\mu$	$e+\text{jets}$	$\mu+\text{jets}$
Correlated					
Primary Vertex	×	×	×	×	×
EM ID	×	×		×	
EM Tracking+Likelihood	×	×		×	
Electron smearing	×	×			
μ ID		×	×		×
μ Tracking		×	×		×
$\mu \chi^2$		×	×		×
μ DCA		×	×		×
μ Isolation		×	×		×
μ smearing		×	×		×
$\Delta z(\ell, PV)$	×	×	×	×	×
Jet ID	×	×	×	×	×
Jet Energy Scale	×	×	×	×	×
Jet Energy Resolution	×	×	×	×	×
L1 EM Trigger	×	×		×	
L3 EM Trigger	×	×		×	
L1 μ Trigger		×	×		×
L2 μ Trigger		×	×		×
L3 jet Trigger				×	×
Jets firing EM trigger	×	×			
Branching fraction	×	×	×	×	×
Z background	×	×	×		
Diboson background	×	×	×		
Uncorrelated					
Likelihood fit W MC model				×	×
Likelihood fit ε_s (e)				×	
Likelihood fit ε_q (e)				×	
Likelihood fit ε_s (μ)					×
Likelihood fit ε_q (μ)					×
gamma conversions		×			
MC statistics	×	×	×	×	×
Template MC statistics				×	×
Statistical uncertainty on the fake rate	×	×	×		

TABLE 3: Summary of the systematic uncertainties affecting different channels. Notation "uncorrelated" and "correlated" refers to the treatment of the sources of errors in the cross section combination.

the cross section changes as a function of m_{top} as:

$$\sigma_{t\bar{t}}(m_{top}) = \sigma_{t\bar{t}} - 0.09 \frac{\text{pb}}{\text{GeV}} \times (m_{top} - 175 \text{ GeV}). \quad (10)$$

B. Lepton+jets channel

The tt production cross sections at $\sqrt{s} = 1.96$ TeV for a top mass of 175 GeV in the $e+\text{jets}$ and $\mu+\text{jets}$ channels are measured to be:

$$\begin{aligned} e + \text{jets} : \quad \sigma_{t\bar{t}} &= 8.2^{+2.1}_{-1.9} (\text{stat})^{+1.9}_{-1.3} (\text{syst}) \pm 0.5 (\text{lumi}) \text{ pb}; \\ \mu + \text{jets} : \quad \sigma_{t\bar{t}} &= 5.4^{+1.8}_{-1.6} (\text{stat})^{+1.2}_{-1.0} (\text{syst}) \pm 0.4 (\text{lumi}) \text{ pb}; \end{aligned}$$

Source	ee	$e\mu$	$\mu\mu$
Primary vertex	± 0.32	± 0.32	± 0.32
EM ID	± 6.5	± 2.5	N/A
EM tracking and likelihood	± 4.7	± 1.9	N/A
Electron smearing	-0.9	-0.5	N/A
μ ID	N/A	± 4.0	± 8.0
μ Tracking	N/A	± 3.0	± 2.4
$\mu \chi^2$	N/A	± 0.1	± 0.2
μ DCA	N/A	± 0.3	± 0.6
μ isolation	N/A	± 0.4	± 0.8
μ smearing	N/A	-0.5	-0.9
$\Delta z(\ell, PV)$	± 0.1	± 0.1	± 0.1
Jet ID	+1.5 -8.7	+5.2 -1.3	+6.5 -1.7
Jet Energy Scale	+6.2 -6.4	+6.5 -5.7	+6.7 -9.1
Jet energy resolution	+2.1	+2.7	+2.3 -0.4
Jet firing EM trigger	± 0.0	+0.3 -0.8	N/A
L1 EM trigger	± 1.1	± 0.02	N/A
L3 EM trigger	± 0.9	± 0.5	N/A
L1 μ trigger	N/A	+3.1 -3.9	+3.0 -3.2
L2 μ trigger	N/A	N/A	+0.1 -0.2
MC Statistics	± 2.8	± 2.2	± 4.8

TABLE 4: Summary of the relative systematic uncertainties (in %) on the $t\bar{t} \rightarrow \ell\bar{\ell}$ signal efficiencies.

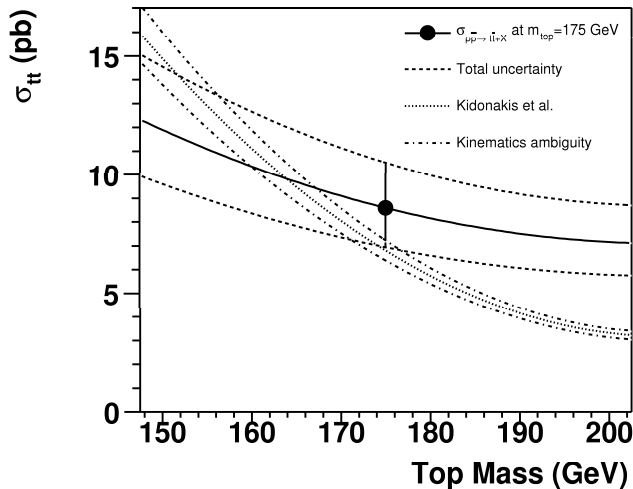


FIG. 1: Combined $t\bar{t}$ production cross section in dilepton channel as a function of top quark mass compared to the theoretical calculations [5]

yielding a combined cross section of

$$\ell + \text{jets} : \quad \sigma_{t\bar{t}} = 6.7^{+1.4}_{-1.3} (\text{stat})^{+1.6}_{-1.1} (\text{syst}) \pm 0.4 (\text{lumi}) \text{ pb.}$$

Table 8 summarizes the contributions from the different sources of systematic uncertainties to the total systematic uncertainty on the cross section in the e +jets, μ +jets and ℓ +jets channels. Figure 2 shows the dependence of the combined cross section in lepton+jets channel on top quark mass. In the region 170 GeV to 180 GeV the cross section changes as a function of m_{top} as:

$$\sigma_{t\bar{t}}(m_{top}) = \sigma_{t\bar{t}} - 0.11 \frac{\text{pb}}{\text{GeV}} \times (m_{top} - 175 \text{ GeV}). \quad (11)$$

Source	ee			e μ			$\mu\mu$		
	WW	Z \rightarrow $\tau\tau$	WW	Z \rightarrow $\tau\tau$	WW	Z \rightarrow $\tau\tau$	WW	Z \rightarrow $\tau\tau$	Z \rightarrow $\tau\tau$
Primary vertex	± 0.32	± 0.32	± 0.32	± 0.32	± 0.32	± 0.32	± 0.32	± 0.32	± 0.32
EM ID	± 7.1	± 7.8	± 2.5	± 2.5	± 2.7	± 2.7	N/A	N/A	N/A
EM tracking and likelihood	± 5.0	± 5.3	± 1.9	± 1.9	± 2.1	± 2.1	N/A	N/A	N/A
μ ID	N/A	N/A	± 4.0	± 4.0	± 4.0	± 4.0	± 8.0	± 8.0	N/A
μ Tracking	N/A	N/A	± 3.0	± 3.0	± 3.0	± 3.0	± 6.0	± 6.0	N/A
μ χ^2	N/A	N/A	± 0.1	± 0.1	± 0.1	± 0.1	± 0.2	± 0.2	N/A
μ DCA	N/A	N/A	± 0.3	± 0.3	± 0.3	± 0.3	± 0.6	± 0.6	N/A
μ isolation	N/A	N/A	± 0.4	± 0.4	± 0.4	± 0.4	± 0.8	± 0.8	N/A
μ smearing	N/A	N/A	-	-	-	-	-2.2	-2.2	+7.9 -10.9
$\Delta z(\ell, PV)$	± 0.1	± 0.1	± 0.1	± 0.1	± 0.1	± 0.1	± 0.1	± 0.1	N/A
Jet ID	-12.9	+24.2 -6.2	+8.6	+7.3 -9.8	-66.6	-66.6	+6.5 -11.8	+6.5 -11.8	N/A
Jet Energy Scale	+28.6 -11.4	+17.6 -32.4	+28.0 -17.7	+18.6 -13.9	+30 -20	+30 -20	+29.8 -16.1	+29.8 -16.1	+31.6 -23.1
Jet energy resolution	-16.7	-32.4	+13.7	-7.3	-66.6	-66.6	+13.3 -2.4	+13.3 -2.4	-18.0
L1 EM trigger	± 1.2	+1.3 - 1.5	± 0.06	± 0.06	± 0.1	± 0.1	N/A	N/A	N/A
L3 EM trigger	± 1.1	± 4.0	± 0.6	± 1.2	± 1.5	± 1.5	N/A	N/A	N/A
L1 μ trigger	N/A	N/A	+3.6 -4.6	+3.4 -4.2	+3.2 -4.0	+3.2 -4.0	+3.3 -3.5	+3.3 -3.5	-0.1
L2 μ trigger	N/A	N/A	N/A	N/A	N/A	N/A	+0.1 -0.2	+0.1 -0.2	± 0.0
Jets firing EM trigger	± 0.0	± 0.0	+0.5 -0.3	+0.6 -0.3	+2.0 -0.0	+2.0 -0.0	N/A	N/A	N/A
Theoretical cross sections/ Normalization	± 35	± 7.5	± 35	± 7.5	± 12.3	± 12.3	± 35	± 35	± 7.5
γ conversion	N/A	N/A	N/A	N/A	± 20.6	± 20.6	N/A	N/A	N/A
MC and fake rate statistics	± 11.8	± 7.7	± 11.7	± 7.7	± 11.7	± 11.7	± 11.7	± 11.7	± 11.7

TABLE 5: Summary of the relative systematic uncertainties (in %) on background.

	e +jets		μ +jets	
	$\Delta\varepsilon$ (%)	ΔN_t^{tt} (%)	$\Delta\varepsilon$ (%)	ΔN_t^{tt} (%)
Primary Vertex	± 1.9	N/A	± 1.7	N/A
EM ID	± 2.4	N/A	N/A	N/A
EM Tracking	± 1.5	N/A	N/A	N/A
EM Likelihood	± 1.8	N/A	N/A	N/A
μ ID	N/A	N/A	± 3.0	N/A
μ Tracking	N/A	N/A	± 3.0	N/A
$\mu \chi^2$	N/A	N/A	± 0.3	N/A
μ DCA	N/A	N/A	± 0.3	N/A
μ Isolation	N/A	N/A	± 0.8	N/A
$\Delta z(\ell, PV)$	± 0.5	N/A	± 0.1	N/A
Jet ID	+7.1-6.5	+4.5-4.7	+5.0-9.3	+3.5-6.9
Jet Energy Scale	+12.4-11.6	-3.2+7.1	+11.2-12.3	-3.6+3.9
Jet Energy Resolution	+1.5+0.4	+2.0+1.6	+0.2-1.7	-1.1-0.4
L1 EM Trigger	+0.0-0.2	+0.0-0.2	N/A	N/A
L2 EM Trigger	± 0.0	± 0.0	N/A	N/A
L3 EM Trigger	± 0.8	± 0.0	N/A	N/A
L1 μ Trigger	N/A	N/A	+4.0-5.0	-0.2+0.3
L2 μ Trigger	N/A	N/A	+4.0-5.5	+0.0-0.1
L1 Jet Trigger	± 0.0	± 0.0	± 0.0	± 0.0
L2 Jet Trigger	± 0.0	± 0.0	± 0.0	± 0.0
L3 Jet Trigger	± 0.0	+0.1-0.2	± 0.1	+0.7-0.8
ε_{sig}	N/A	-0.1+0.1	N/A	-0.2+0.1
ε_{QCD}	N/A	-3.3+3.1	N/A	-1.1+0.9
W MC Modeling	N/A	+2.1-2.1	N/A	± 8.0
MC Statistics	± 1.5	N/A	± 1.9	N/A
Template Statistics	N/A	± 5.5	N/A	± 4.5

TABLE 6: Summary of the relative systematic uncertainties on the $t\bar{t}$ preselection efficiency and on the number of fitted $t\bar{t}$ events.

C. Combined cross section

The combined $t\bar{t}$ production cross sections at $\sqrt{s}=1.96$ TeV for a top mass of 175 GeV in the ℓ +jets and dilepton channels is measured to be:

$$\text{combined} : \quad \sigma_{t\bar{t}} = 7.1_{-1.2}^{+1.2} (\text{stat}) \quad {}_{-1.1}^{+1.4} (\text{syst}) \pm 0.5 (\text{lumi}) \text{ pb.}$$

Table 9 summarizes the contributions from the different sources of systematic uncertainties to the total systematic uncertainty on the cross section in the dilepton, lepton+jets and combined channels.

Figure 3 shows the dependence of the combined cross section in lepton+jets channel on top quark mass. In the region 170 GeV to 180 GeV the cross section changes as a function of m_{top} as:

$$\sigma_{t\bar{t}}(m_{top}) = \sigma_{t\bar{t}} - 0.1 \frac{\text{pb}}{\text{GeV}} \times (m_{top} - 175 \text{ GeV}). \quad (12)$$

Figure 4 shows the summary of the cross section measurements in different channels along with the current combined cross section and the theoretical prediction.

Channel	ee	$e\mu$	$\ell\ell$
correlated			
Primary Vertex	± 0.05	± 0.03	± 0.03
EM ID	$-1.0+1.1$	$-0.26+0.27$	$-0.25+0.27$
EM Tracking+Likelihood	$-0.72+0.79$	$-0.20+0.21$	$-0.19+0.20$
Electron smearing	$-0+0.14$	$-0+0.05$	$-0+0.04$
μ ID	N/A	$-0.41+0.44$	$-0.38+0.41$
μ Tracking	N/A	$-0.31+0.33$	$-0.22+0.23$
$\mu \chi^2$	N/A	± 0.01	± 0.01
μ DCA	N/A	± 0.03	± 0.03
μ Isolation	N/A	± 0.04	± 0.04
μ smearing	N/A	$-0+0.05$	$-0+0.04$
$\Delta z(\ell, PV)$	± 0.02	± 0.01	± 0.01
Jet ID	$-0.33+1.52$	$-0.55+0.19$	$-0.49+0.30$
Jet Energy Scale	$-1.09+1.25$	$-0.81+0.75$	$-0.74+0.79$
Jet Energy Resolution	$-0.31+0.24$	$-0.32+0.05$	$-0.26+0.12$
L1 EM Trigger	$-0.17+0.18$	± 0.003	± 0.02
L3 EM Trigger	± 0.16	± 0.06	± 0.05
L1 μ Trigger	N/A	$-0.32+0.44$	$-0.24+0.31$
L2 μ Trigger	N/A	N/A	$-0.002+0.004$
Jets firing EM trigger	N/A	$-0.03+0.08$	$-0.02+0.05$
Branching fraction	$-0.29+0.30$	$-0.19+0.20$	$-0.17+0.18$
Z background	± 0.04	± 0.04	± 0.04
Diboson background	± 0.18	± 0.17	± 0.17
Uncorrelated			
MC and fake rate statistics	$-0.57+0.59$	$-0.23+0.24$	± 0.2
gamma conversions	± 0.004	± 0.006	± 0.005
TOTAL	$-1.8+2.5$	$-1.3+1.2$	$-1.1+1.1$

TABLE 7: Summary of the effect of systematic uncertainties on single channels (ee and $e\mu$) and the combination result in dilepton channel ($\Delta\sigma_{t\bar{t}}$ in pb).

-
- [1] C. Clement *et al.* *Measurement of the $t\bar{t}$ Production Cross-Section at $\sqrt{s} = 1.96$ TeV in the Electron+Jets Final State using a Topological Method*, DØ Note 4662, December 2004.
- [2] T. Golling *Measurement of the $t\bar{t}$ Production Cross-Section at $\sqrt{s} = 1.96$ TeV in the Muon+Jets Final State using a Topological Method*, DØ Note 4667, December 2004.
- [3] S. Anderson, *et al.* *Measurement of the $t\bar{t}$ Production Cross-Section at $\sqrt{s} = 1.96$ TeV in Dilepton Final States*, DØ Note 4683, January 2005.
- [4] S. Eidelman *et al.*, *Phys. Lett. B* **592**, 1 (2004).
- [5] R. Bonciani *et al.*, *Nucl. Phys. B* **529**, 424 (1998); N. Kidonakis and R. Vogt, *Phys. Rev. D* **68**, 114014 (2003); M. Cacciari *et al.*, *JHEP* **404**, 68 (2004).
- [6] The original code for the cross section combination has been provided by Arnulf Quadt.

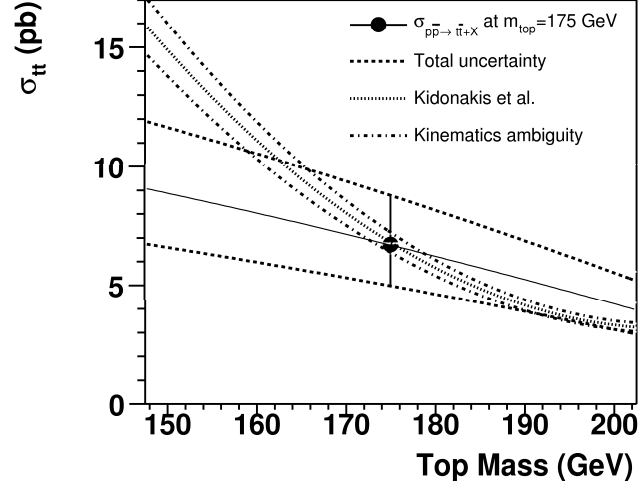


FIG. 2: Combined $t\bar{t}$ production cross section in lepton+jets channel as a function of top quark mass compared to the theoretical calculations [5]

Channel	e +jets	μ +jets	ℓ +jets
correlated			
Primary Vertex	-0.16+0.16	± 0.09	-0.12+0.13
EM ID	-0.20+0.21	N/A	± 0.07
EM Tracking+Likelihood	-0.19+0.20	N/A	± 0.07
μ ID	N/A	-0.16+0.17	-0.11+0.12
μ Tracking	N/A	-0.16+0.17	-0.11+0.12
μ χ^2	N/A	± 0.02	± 0.01
μ DCA	N/A	± 0.02	± 0.01
μ Isolation	N/A	± 0.04	± 0.03
$\Delta z(\ell, PV)$	± 0.04	± 0.005	± 0.02
Jet ID	-0.20+0.16	-0.08+0.14	-0.11+0.19
Jet Energy Scale	-1.18+1.78	-0.73+1.01	-0.95+1.43
Jet Energy Resolution	+0.04+0.10	-0.07+0.07	+0.01+0.12
L1 EM Trigger	± 0.00	N/A	± 0.00
L3 EM Trigger	-0.07+0.07	N/A	-0.02+0.03
L1 μ Trigger	N/A	-0.22+0.30	-0.16+0.20
L2 μ Trigger	N/A	-0.21+0.31	-0.15+0.21
L1 Jet Trigger	± 0.00	± 0.00	± 0.00
L3 Jet Trigger	+0.01-0.02	+0.03-0.04	± 0.02
Branching fraction	-0.16+0.17	± 0.10	-0.13+0.14
W MC Modeling	± 0.18	± 0.44	± 0.29
uncorrelated			
Likelihood fit $\varepsilon_{sig}(e)$	± 0.01	N/A	± 0.005
Likelihood fit $\varepsilon_{QCD}(e)$	-0.27+0.26	N/A	-0.15+0.14
Likelihood fit $\varepsilon_{sig}(\mu)$	N/A	± 0.01	-0.005+0.004
Likelihood fit $\varepsilon_{QCD}(\mu)$	N/A	± 0.03	± 0.017
MC Statistics	± 0.46	± 0.24	± 0.24
TOTAL	-1.3+1.9	-1.0+1.2	-1.1+1.6

TABLE 8: Summary of the effect of systematic uncertainties on single channels and the combination result in ℓ +jets channel ($\Delta\sigma_{t\bar{t}}$ in pb).

Channel	combined
Primary Vertex	± 0.11
EM ID	± 0.11
EM Tracking+Likelihood	± 0.09
Electron smearing	-0 +0.006
μ ID	-0.16+0.17
μ Tracking	-0.13+0.14
$\mu \chi^2$	± 0.01
μ DCA	± 0.01
μ Isolation	± 0.03
μ smearing	-0 +0.007
$\Delta z(\ell, PV)$	± 0.02
Jet ID	-0.20+0.24
Jet Energy Scale	-0.91+1.28
Jet Energy Resolution	-0.04+0.12
L1 EM Trigger	-0.003+0.002
L3 EM Trigger	± 0.03
L1 μ Trigger	-0.17+0.22
L2 μ Trigger	-0.13+0.17
L3 jet Trigger	-0.02+0.01
Jets firing EM trigger	-0.004+0.008
gamma conversions	± 0.001
Branching fraction	-0.14 +0.15
Z background	± 0.01
W background	± 0.04
Likelihood fit W MC model	± 0.22
Likelihood fit $\varepsilon_{sig}(e)$	-0.001+0.004
Likelihood fit $\varepsilon_{QCD}(e)$	-0.11+0.10
Likelihood fit $\varepsilon_{sig}(\mu)$	-0.004+0.003
Likelihood fit $\varepsilon_{QCD}(\mu)$	± 0.01
MC and fake rate statistics	± 0.14
TOTAL	-1.1+1.4

TABLE 9: Summary of the effect of systematic uncertainties on the combination result ($\Delta\sigma_{t\bar{t}}$ in pb).

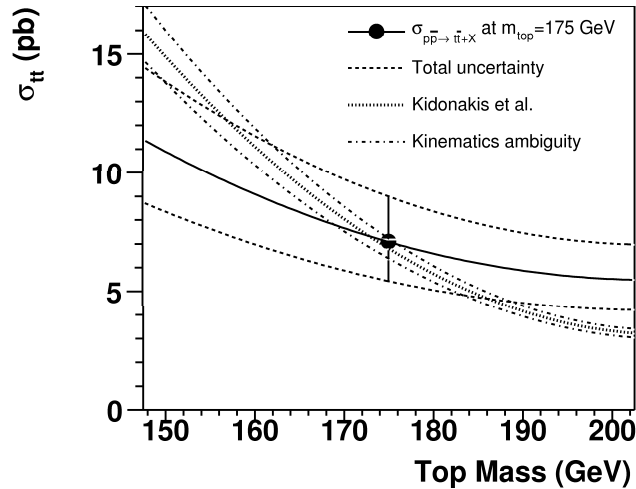


FIG. 3: Combined $t\bar{t}$ production cross section as a function of top quark mass compared to the theoretical calculations [5]

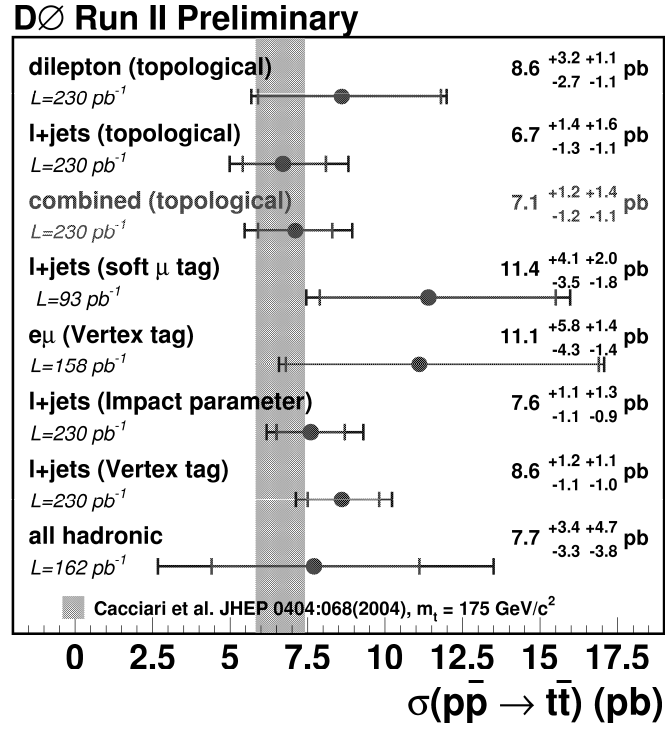


FIG. 4: $t\bar{t}$ production cross section summary compared to the theoretical calculations